

## Module 4 : Third order nonlinear optical processes

### Lecture 31 : Coherent anti-Stokes Raman scattering

#### Objectives

#### In this lecture you will learn the following

- This lecture will focus on the basic principle of Coherent anti-Stokes Raman scattering spectroscopy.

#### Coherent anti-Stokes Raman scattering

Coherent anti-Stokes scattering was first observed by Maker and Terhune. In this process, the beat frequency of two incident waves at frequencies  $\omega_1$  and  $\omega_2$  ( $\omega_1 > \omega_2$ ) coherently excites the material excitation wave  $\omega_m = \omega_1 - \omega_2$  which is then mixed with  $\omega_1$ , to produce a coherent field at  $\omega_{as} = 2\omega_1 - \omega_2$  as depicted in figure 31.1.

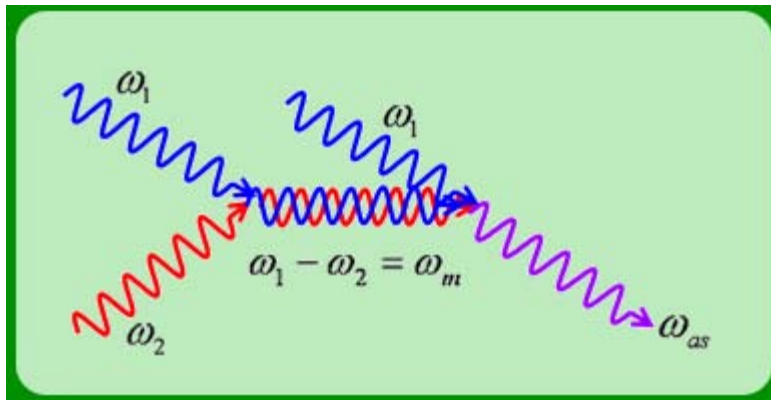


Figure 31.1

Figure 31.2 presents the quantum mechanical transition scheme.

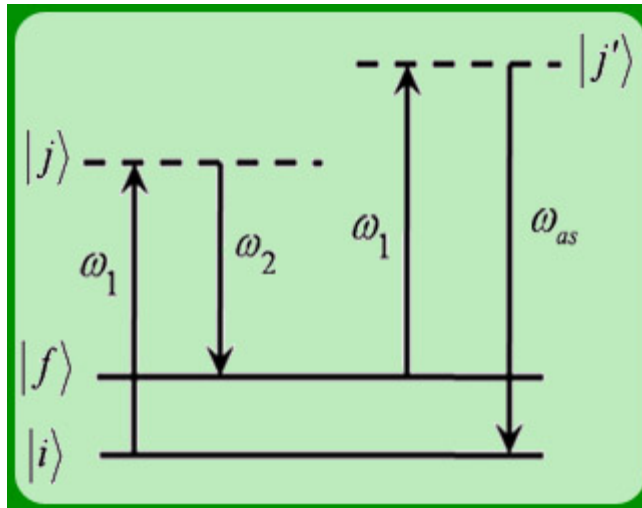


Figure 31.2

It is thus an example of a four-wave-mixing process and can be regarded as the coherent version of spontaneous Raman scattering. Since all the Raman active transitions can be accessible in this process. It constitutes one of the most powerful nonlinear spectroscopic techniques.

The output is produced by nonlinear polarization which is a consequence of  $\chi_{xxx}^{(3)}(-\omega_{as}, \omega_1, \omega_2, \omega_s)$  given by.

$$\chi_{\text{osc}}(\omega_{\text{as}}) = -\frac{A}{2\omega_m((\omega_1 - \omega_2) - \omega_m + i\gamma)} \quad (31.1)$$

An inspection of this equation reveals that  $\chi_{\text{osc}}(\omega_{\text{as}})$  will exhibit resonant enhancement when the input field frequencies are tuned such that  $\omega_1 - \omega_2 = \omega_m$ . Under condition of resonance, the large signal wave can be generated even with low pump intensities.

Further, the output is coherent and highly directional which simplifies the signal collection issues. For these reasons it has sensitivity high enough for the trace chemical analysis

and studies on material structure as  $\omega_m$  and  $\gamma$  have sensitive dependence on the molecular chemical environment. Further, the transient CARS with ultrafast lasers pulses  $\sim 1\text{ps}$ , can reveal the transient species in a chemical reaction.

The generation of anti-Stokes signal is described any of the coupled differential equations (30.17) and (30.18) in lecture#30. We again write here the equation for the spatial evolution of  $E_{\text{as}}$ .

$$\frac{dE_{\text{as}}}{dz} = -\alpha_{\text{as}} E_{\text{as}} + \kappa_{\text{as}} E_2^* e^{i\Delta k z} \quad (31.2)$$

where

$$\alpha_{\text{as}} = \frac{-3i\omega_{\text{as}}}{n_{\text{as}}c} \chi_R |E_1|^2 \quad (31.3)$$

$$\kappa_{\text{as}} = \frac{3i\omega_{\text{as}}}{2n_{\text{as}}c} \chi_{\text{osc}} E_1^2 \quad (31.4)$$

and

$$\Delta k = \Delta \vec{k} \cdot \vec{z} = (2\vec{k}_1 - \vec{k}_2 - \vec{k}_{\text{as}}) \cdot \hat{z} \quad (31.5)$$

CARS signal is studied generally under the condition that the second term dominates in equation (31.2) i.e. SRS gain is small. Since the material resonance reflected in where resonance character of  $\chi_{\text{osc}}$ , the spectral profile is expected to be Lorentzian. A typical CARS signal is shown in figure 31.3 and it can be seen that it is not the case.

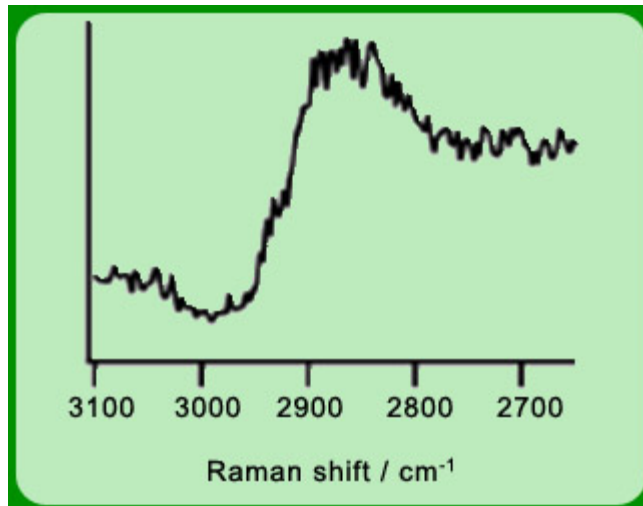


**Figure 31.3**

This is so because in addition to the resonant molecular response generated by  $\chi_{\text{osc}}$ , material also possess nonresonant susceptibility  $\chi_{\text{NR}}^{(3)}$  of the electronic and vibrational origin. The CARS signal is then

governed by  $\chi_{\text{total}}^{(3)} = \chi_{\text{NR}}^{(3)} + \chi_{\text{osc}}^{(3)}$  and can be written as

$$S(\omega_s) \propto \left| \chi_{NR}^{(3)} + \chi_{sax}^{(3)} \right|^2$$

$$\propto \left[ \chi_{NR}^{(3)} + \frac{A(\omega_1 - \omega_2 - \omega_m)}{(\omega_1 - \omega_2 - \omega_m)^2 + \gamma^2} \right]^2 + \frac{A^2 \gamma^2}{((\omega_1 - \omega_2 - \omega_m)^2 + \gamma^2)^2} \quad (31.6)$$

which is asymmetric with respect to the resonance point with a peak and a valley structure at

$$(\omega_1 - \omega_2)_+ + (\omega_1 - \omega_2)_- = \left( \frac{A}{\chi_{NR}^{(3)}} \right)^2 + 4\gamma^2 \quad (31.7)$$

$\Rightarrow$

$$(\omega_1 - \omega_2)_+ + (\omega_1 - \omega_2)_- = 2\omega_m - \frac{A}{\chi_{NR}^{(3)}} \quad (31.8)$$

and

$$(\omega_1 - \omega_2)_+ + (\omega_1 - \omega_2)_- = \left( \frac{A}{\chi_{NR}^{(3)}} \right)^2 + 4\gamma^2 \quad (31.9)$$

Measurement of  $(\omega_1 - \omega_2)_\pm$  and corresponding intensities thus enable, in principle, to determine  $\omega_m$ ,  $A$ ,  $\gamma^2$  and  $\chi_{NR}^{(3)}$  from equations (31.8) and (31.9). However, inaccuracies in the intensity measurements, does not allow accurate determination but only estimates of these quantities. A typical CARS experimental setup is shown in figure 31.4. The signal collection direction is determined from the phase matching condition mentioned in lecture #30. For eliminating the nonresonant  $\chi_{NR}^{(3)}$  contribution to the signal, one can use another variant- Polarization CARS.

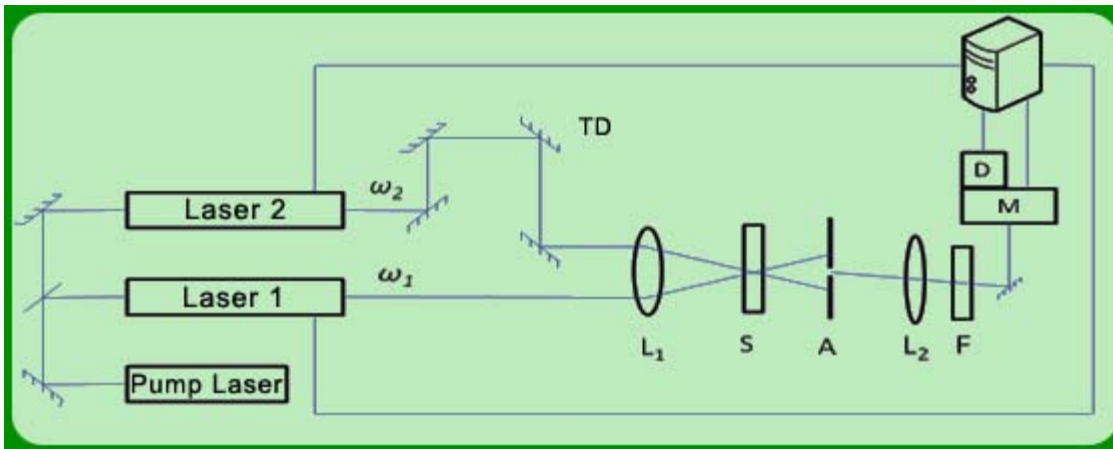


Figure 31.4 TD-Time Delay; L<sub>1,2</sub>-Lens; S-Sample; A-Aperture; M-Monochromator; D-Detector; F-Filter

### Recap

In this lecture you have learnt the following

- Will focus on the basic principle of Coherent anti-Stokes Raman scattering.
- Structure of CARS signal and
- Experimental setup CARS.